
Article:
Stephen, J., Marshall, M. and Lewis, R. (2017) Relaxation of contact pressure and self-loosening in dynamic bolted joints. Proceedings of the Institution of Mechanical Engineers, Part C: Journal of Mechanical Engineering Science, 231 (18). pp. 3462-3475. ISSN 0954-4062

https://doi.org/10.1177/0954406216645130

Relaxation of contact pressure and self loosening in dynamic bolted joints

JT Stephen, MB Marshall and R Lewis

Department of Mechanical Engineering, The University of Sheffield, Mappin Street, Sheffield S1 3JD, UK

Corresponding author:

Stephen Joseph Temitope, Department of Mechanical Engineering, The University of Sheffield, Mappin Street, Sheffield, S1 3JD, UK.
Email: mep10tjs@sheffield.ac.uk

Abstract

Bolted joints are widely used in a variety of engineering applications where they are dynamically loaded with frequencies of vibration spread over a wide spectrum with the same general effects. When under dynamic loading, bolted joints can become loose due to a loss in clamping pressure in the joints. This vibrational loosening sometimes can cause serious problems, and in some cases can lead to fatal consequences if it remains undetected. Non-intrusive ultrasonic and image processing techniques were simultaneously used to investigate the relaxation of contact pressure and loosening of bolted joints subjected to cyclic shear loading. Three critical areas: the contact interface of the bolted component, the bolt length and the rotation of the bolt head were monitored during loosening of the joints. The results show that loosening of bolted joints can be grouped into three stages of: very rapid, rapid and gradual loosening. The earliest stage of the loosening of bolted joints is characterised by cyclic strain ratcheting- loosening of the bolted joint during vibration without rotation of the bolt head. The higher the rate of relaxation at this early stage, the lower is the resistance of the bolted joint to vibration induced loosening. Both the dynamic shear load and an additional constant shear load in another direction was observed to affect the rate of loosening at this early stage, a rise in the magnitude of the additional constant shear load increases the rate of loosening. Furthermore, the contact pressure distribution affects the rate of loosening at the bolted joint interface, as loosening increases away from area of high contact pressure.

KEY WORDS
Bolted joints, cyclic shear load, contact pressure, self-loosening, ultrasonic technique.

Introduction

One of the major advantages of threaded fasteners over other fastening methods which leads to their wide use in modern engineering structures and machine design is that the joint components can easily be assembled and disassembled, and also re-used (especially for maintenance purposes). However, they sometimes fail in operation by loosening when subjected to dynamic loads [1, 2]. In some cases, these failures are of fatal consequence, and hence, they are safety critical [3-5]. In order to prevent loosening, various techniques and locking devices are used. Studies conducted to assess the performance of these locking devices have shown that the majority of them do not totally lock the fastener, but tolerate some degree of self-loosening under dynamic shear loading [6, 7].

Attempts have been made by several studies to satisfactorily understand self-loosening of bolted joints subjected to vibrating shear loads with each having limited success. The earliest research works were focused on bolted joints loosening as a consequence of circumferential dilation of the nut and contraction of the bolt as a result of vibration loading in the axial direction of the fasteners [8, 9]. However, Gerhard H. Junker in 1960 showed that self-loosening induced by transverse vibration perpendicular to the thread axis is a major cause of failure in bolted joints. Loosening was attributed to slip at the fasteners surfaces due to a reduction in clamping friction caused by the applied shear load. Recently, studies have attributed the initiation of self-loosening due to transverse vibration to a reduction in friction and clamping force due to accumulation of localized slip in the form of strain at the fastener contact surfaces [10-12]. Experimental research reports have also shown the dependence of loosening life on the preload for different values of initial preload, frequency, thread pitch and prevailing torque [13-16].

In most of these studies, the loosening of bolted joints was decided by the amount of pre-torque remaining in the joint, and some of the techniques applied include torque control methods through a calibrated wrench, extension control using ultrasonic methods to monitor the extension of the bolt which was then calibrated to torque and impedance based techniques using embedded piezo-electric elements for damage detection in structural health monitoring of bolted joints [17-19]. One of the disadvantages of some of these techniques was that they cannot be used to gather information from contacting surfaces. Except in the ultrasonic studies conducted by Marshall et al. and through the use of Lamb waves by Yang and Change, measurements were restricted to the threaded fasteners in the techniques that can be used to collect data during test setup. They failed to gather information from the clamped interface, which is a critical element of the bolted joint. Furthermore, in some of the experimental studies, bolted joint components and the contact interface were modified, and this presents issues as they may not now actually represent the true operating conditions of bolted joints [13, 20, 21]. While in service, bolted joints are subjected to additional shear loads in other directions to the cyclic shear load and such loads were also previously ignored.

Previously, non-intrusive ultrasonic techniques have been used to study contact pressure distribution at the clamped interface of unmodified bolted joints [22, 23], and Marshall et al. [15] have proved that ultrasonic reflections from the clamped interface could be used to assess the progress of relaxation in bolted joints. Although, this study, like most of the others studies, only concentrated on one area of the bolted joints, and measurement was limited to a few discrete points of the bolted plate interface. Therefore, the present study intends to explore this technique further to study the loosening of the bolted joints. Changes in the tension in the bolt and rotation of the bolt head, in addition to the change in the contact pressure at the clamped interface of bolted joints subjected to varying bolt torque, cyclic shear load and additional transverse load will be monitored with the intention to understand the mechanisms of bolted joint loosening, and also to establish a practical condition monitoring technique for bolted joints.

Rough Surface Contact and Ultrasound

Contact surfaces in bolted joints like in other engineering surfaces are not perfectly smooth. They exhibit surface roughness, which is manifested in the form of surface waviness and asperities, and this is evident when observed under a microscope [18]. Therefore, when two rough surfaces are loaded together they mostly interact at the junctions of the surface roughness/asperities, with air gaps at the void between the asperities. When normal ultrasound waves are incident at a joined interface, the waves are partially reflected at the interface (Figure 1a). Sound is transmitted at the asperity junctions, and reflected at the metal-air interface due to the trapped air pockets. How much sound is transmitted depends on the wavelength of the sound wave relative to the air gap.

The proportion of ultrasound wave incident at the interface that is reflected from it is known as the reflection coefficient for displacement wave amplitude, *R*, and is given as:

$$R = \frac{z_1 - z_2}{z_1 + z_2} \qquad 1$$

where z is the acoustic impedance and subscripts 1 and 2 refer to acoustic impedance for the material on either side of the interface. The acoustic impedance is equal to product of wave speed and density for a given material.

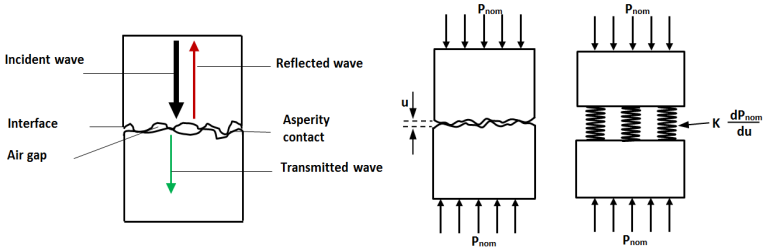

Figure 1: (a) Ultrasonic reflection at a rough surface interface and (b) Schematic representation of an interface using the spring model

In a study conducted by Kendall and Tabor [19] on rough surface contacts, and followed up by Tattersall [20] on adhesive layers, the asperity interactions of the interface were modelled as a series of parallel springs (Figure 1b). They found out that the reflection coefficient depends on the interfacial stiffness, K, and for a homogenous contact with two similar materials, the relationship between them is reduced to and governed by the relationship:

$$|R| = \frac{1}{\sqrt{1+(2K/\omega z)^2}} \qquad 2$$

where ω is the angular frequency of the sound wave. The interfacial stiffness, which is expressed per unit area, is defined as the change in nominal contact pressure, P_{nom}, required to cause unit approach of the mean lines of two surfaces. Thus:

$$K = -\frac{dP_{nom}}{du} \qquad 3$$

where u is the separation of the mean lines of roughness of the two surfaces. Interfacial stiffness for a given pair of contacting surfaces varies from zero when surfaces are just touching (the asperities can easily be deformed and separation between surfaces can be reduced) to infinity when surfaces are completely conformal (deformation of asperities and reduction of separation between surfaces is no longer possible). The stiffness depends on distribution, size and number of asperity junctions. Thus, its value is partially linear and depends on applied load, with no single relation between it and contact pressure. However, a relationship between the contact pressure and the interfacial stiffness was explored by Dwyer-Joyce and Drinkwater [21] through a calibration experiment. At low applied loads, Arakawa [23] and Hodgson *et al.* [24] showed that this relationship is linearly proportional. Furthermore, study conducted by Drinkwater *et al.* [22] showed that the spring model could be applied to reflection data from rough surface interfaces for ultrasound frequencies up to a maximum of 50 MHz, depending on the materials and surface roughness of the contact under investigation.

Experimental Procedure

Test specimens and ultrasonic instrumentation

The bolted joint specimens were manufactured from EN24 steel and clamped together with an M12 (grade 8.8) steel bolt. The front plate of the specimen had a clearance hole of 13.5 mm diameter through it while the back plate had a blind threaded hole of 8 mm screw-in depth. The contact surfaces of both plates were ground to an average surface roughness of 0.5 μm (Ra). The contact surface area between the plates when bolted was approximately 2947 mm^2. The back plate (Plate A) was to have the piezoelectric transducers mounted on the under-side of it, while a transducer would be attached to the top of the bolt. A 5 mm diameter hole was also drilled through Plate B parallel to the centre of the clearance hole. This was to allow for the introduction of additional transverse side loads to the dynamic shear load acting on the bolted joint during the experiments. The bearing friction coefficient under the bolt head was approximately 0.15, while the friction coefficient between the threads and the friction coefficient between the clamped plates were approximately 0.17 and 0.15 respectively. These values were estimated using data from standard reciprocating friction tests from the respective interfaces considered.

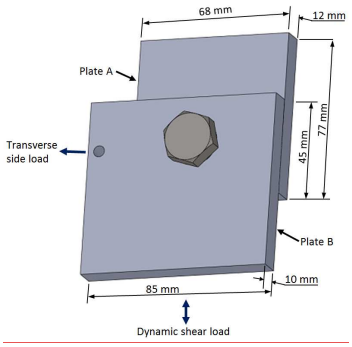

Figure 2: Test specimen (plates and bolt)

The piezoelectric (lead zirconate titanate) transducers used in this study had a centre frequency of 10 MHz, thickness of 0.2 mm and were cut to form strips of 2 mm × 1 mm active area in order to maximise spatial resolution. When excited, they emitted a gradually diverging ultrasonic sound wave approximately equal to the dimension of the sensors' active area. A transducer of 5 mm × 1 mm active area was cut for the bolt head. The transducers were permanently bonded directly to the back of the plate with the threaded hole and the bolt head using *M-bond 610* (*Vishay*) adhesive.

The design and placement of the transducer array on the back of the plate with the threaded hole was dictated by the result of the measured contact pressure map of a static bolted joint (Figure 3(a)). A static scan was performed on the bolted joint specimen with a bolt torque of 50 Nm using a 10 MHz focusing transducer. The specimen was mounted in a scanning tank, and the ultrasonic signal focused on the interface of interest using a water couplant. The scan was performed on a square area of 40 mm × 40 mm at a resolution of 0.25 mm and 0.125 mm steps in the x and y directions respectively. A reference scan was also produced when the

plate B was removed. The reflection coefficient map was obtained by dividing the reflected voltage of the loaded joint with the reference on a point by point basis. By doing this, the effect of attenuation on the signals in the plate is removed leaving only the reflection coefficient, which represents the fraction of ultrasound incidence at the interface that is reflected from it. This was used to produce the map of interfacial stiffness using Equation 2, and a calibration experiment used to determine contact pressure. Further details on this procedure and calibration experiment are provided in Stephen et al. [23]. As seen in Figure 3a, the pressure distribution map has peak pressures located very close to the edge of the bolt hole and this pressure diminishes as the distance from the edge of the bolt hole increases.

As shown in the layout in Figures 3 (b), the sensors were grouped into four sets of eight transducers, and transducers in each group were numbered from 1 to 8. All transducers with identical number in all the groups were positioned at the same radial distance from the edge of the bolt hole. In all the groups, transducers numbered 1 and 5, 3 and 7, 2 and 6, and 4 and 8 were respectively positioned at radial distances of 7 mm, 8 mm, 9 mm and 10 mm from the bolt centre. The transducers were evenly distributed around the threaded hole with each sensor separated, circumferentially, by an angle of 22.5^0 from adjacent transducers. Furthermore, for each of the transducers, the longer dimension was placed in the circumferential direction as this will maximise the resolution of the sensor in the radial direction. The transducers occupied a small annulus area of approximately 265 mm^2 around the bolt hole. Figures 3(c) and 3(d) show the bonded transducer array on the plate A and a transducer on the bolt head. Coaxial data wires were soldered to the terminals of the transducers. The transducers along with the wire at the soldered point were then covered with epoxy resin to protect it from damage during handling.

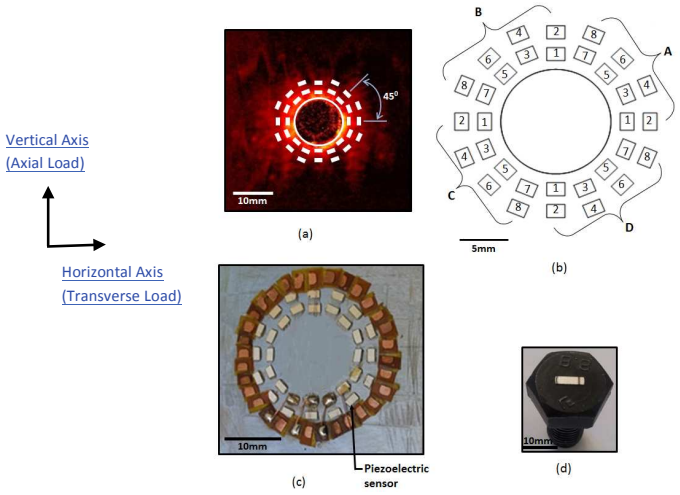

Figure 3: (a) Map of a scan of a static bolted joint with the 32 transducer array; (b) Layout of transducers with identifying numbers and groups; (c) Glued transducers on the plate and (d) Glued transducer on the bolt head

Data acquisition equipment and test rig

The equipment used to generate and receive ultrasonic signals for the tests consists of a PC (FMS100 System) fitted with an ultrasonic pulser-receiver (UPR), digitiser and multiplexer cards. This was used to pulse and measure ultrasonic reflections from the clamped interface through the 32 sensor array, and also to measure ultrasonic reflection from the end of the bolt by the sensor on the bolt head. A camera was positioned facing the bolt head to capture the rotation of the bolt head during the vibration loosening experiment (Figure 4).

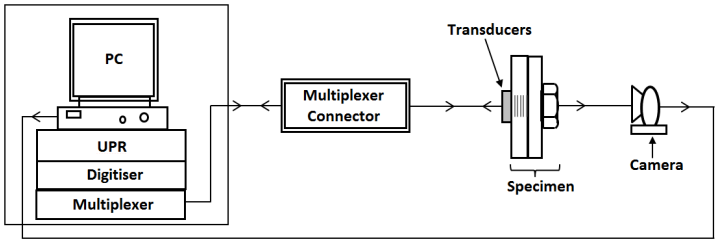

Figure 4: Schematic diagram of ultrasonic equipment

Under the image processing technique, acquisition and processing were done using Matlab image processing toolbox [24]. Three markers of different colours (blue, red and green) of 3 mm diameters were used. Two were placed at the centre and the edge of the bolt head, while the remaining one was placed at a spot on the clamped plate (Figure 5). The images of the markers were captured at a set time interval by the camera. A combination of RGB and L*a*b colour conversion were employed to identify the colours, and the locations of the midpoints of the makers in each captured image were then determined. The angle α of each image during the test was calculated using the cosine rule. This was used to map the rotation of the bolt during relaxation of the joint during the tests by calculating the different between angle α of the captured image at a particular point in time and the calculated angle of the first image.

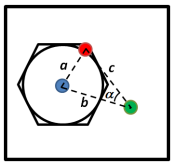

Figure 5: Schematic diagram of the bolt head with markers

The rig was designed in such a way that the upper plate of the joint was held in a fixed position while the lower plate was constrained to a sliding motion in the horizontal direction, and vibratory motion was possible in the vertical direction (Figure 6 shows the desired constraints and the degrees of freedom).

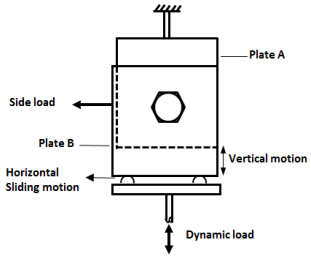

Figure 6: Schematic diagram of the bolted joint experimental set-up

Test procedure

The M12 instrumented bolt with a clamp length of 10 mm was placed in position and torqued up to the required load using a digital torque wrench with a calibrated accuracy of ±2% after the plate specimens had been assembled on the test rig. Bolt torques of 30 Nm, 40 Nm, 50 Nm and 60 Nm which correspond to preloads of 9.4 kN, 12.5 kN, 15.6 kN and 18.6 kN respectively were applied on the joints [25]. The values of preload selected were significantly lower than the proof load (78.8 Nm), and in keeping with similar studies, were chosen in order to avoid saturation of the interface pressure distribution and to explore the effect of its variation on relaxation. Markers were placed in position on the M12 bolt head and bottom plate. The camera was then placed in position and all connections between the sensors and the PC were then made. During the test, cyclic loads with a sinusoidal displacement cycle with a maximum of 0.75 mm were applied to the bolted joint through a hydraulic actuator while the pneumatic actuator applied side loads to the joint when required. Loads from both actuators were monitored and controlled with the help of the installed load cells. A limit was placed on the test duration; if the joint did not loosen after 300 seconds the test was stopped. Additionally, a thin layer of grease was applied to the joint contact surfaces, with these latter two measures taken to minimise the effects of fretting wear on the specimen.

Ultrasonic monitoring of the bolted joint interface was performed with each of the transducers excited with a 25 *V* 'top-hat' signal of 100 ns duration with a pulser repetition rate of 1 kHz. The reflected signals from the interface were digitised with *12-bit* resolution at a rate of 100 million samples per second. The digitised reflected signals were recorded for post processing. Prior to each test, a reference measurement for each of the sensors was recorded with the plate B absent. As previously detailed, the reference measurement is carried out in order to create a metal-air interface so that the entire ultrasonic signal will be reflected. The reference along with the reflected signals obtained during the test when the joints were undergoing loosening would be then used to produce the reflection coefficient. The camera was set to take an image of the bolt head and top plate every second, and the images acquired were stored on a PC and later post-processed to determine the rotation of the bolt head during the test. In all the tests, a washer was placed under the bolt head to ensure a pressure distribution at the interface predominately independent of bolt head rotational position, thus removing a potential source of variation in the experimental set-up. Table 1 shows tests performed on the bolted joints.

Matt Marshall 17/2/2016 09:04
Deleted: A

Matt Marshall 17/2/2016 09:04
Deleted: b

Stephen 29/1/2016 05:09
Formatted: Font:+Theme Body, 10 pt, Not Italic

Stephen 29/1/2016 05:09
Formatted: Font:+Theme Body, 10 pt, Not Italic

Stephen 29/1/2016 05:09
Formatted: Font:+Theme Body, 10 pt, Not Italic

Matt Marshall 17/2/2016 09:05
Deleted: s

Matt Marshall 17/2/2016 09:04
Deleted: to

Stephen 29/1/2016 05:09
Formatted: Font:+Theme Body, 10 pt, Not Italic

Stephen 29/1/2016 05:09
Formatted: Font:+Theme Body, 10 pt, Not Italic

Matt Marshall 17/2/2016 09:04
Deleted: preloads

Stephen 29/1/2016 05:09
Formatted: Font:+Theme Body, 10 pt, Not Italic

Matt Marshall 17/2/2016 09:25
Formatted: Font:10 pt

Matt Marshall 17/2/2016 09:06
Deleted: amplitude

Matt Marshall 17/2/2016 09:06
Deleted: sinusoidal displacement cycle

Stephen 28/1/2016 16:05
Formatted: Font:10 pt

Stephen 28/1/2016 16:05
Formatted: Font:10 pt

Stephen 28/1/2016 16:05
Formatted: Font:10 pt

Matt Marshall 17/2/2016 09:07
Deleted:

Matt Marshall 17/2/2016 09:07
Deleted: to increase the clamping integrity of the joint

Table 1: Loosening tests performed on the dynamic bolted joints

S/No	Torque (Nm)	Cyclic shear load (kN)	Frequency (Hz)	Constant shear load (kN)
Torque				
1	30	6.0	1	0
2	40	6.0	1	0
3	50	6.0	1	0
4	60	6.0	1	0
Cyclic shear load				
1	50	5.5	1	0
2	50	6.0	1	0
3	50	6.5	1	0
4	50	7.0	1	0
5	50	7.5	1	0
6	50	8.0	1	0
Constant shear load				
1	50	6.0	1	0
2	50	6.0	1	1
3	50	6.0	1	2
4	50	6.0	1	3
5	50	6.0	1	4

Stephen 28/1/2016 16:05
Formatted: None, Space Before: 0 pt, Don't keep with next, Don't keep lines together

Stephen 28/1/2016 16:05
Formatted: None, Space Before: 3 pt, Don't keep with next, Don't keep lines together

Stephen 28/1/2016 16:06
Formatted: None, Space Before: 3 pt, Don't keep with next, Don't keep lines together

Results

Figure 7 (a) shows an example of a measured reflected and reference signal from the bolted interface, isolated in the time domain. The dynamic reflection coefficient (RC) of the reflected ultrasonic signals from the interface for each of the dynamic tests was calculated by dividing the reflected signal during the loosening test by the reference signal. Figure 7 (b) represents results of the raw data from a group of 8 sensors that were designed to monitor the contact pressure at the plates interface, while Figure 7 (c) shows the dynamic time of flight measurement measured by the sensor on the bolt head which indicates the relaxation of tension in the bolt during the test.

Stephen 28/1/2016 16:18
Deleted: a

Stephen 28/1/2016 16:18
Deleted: b

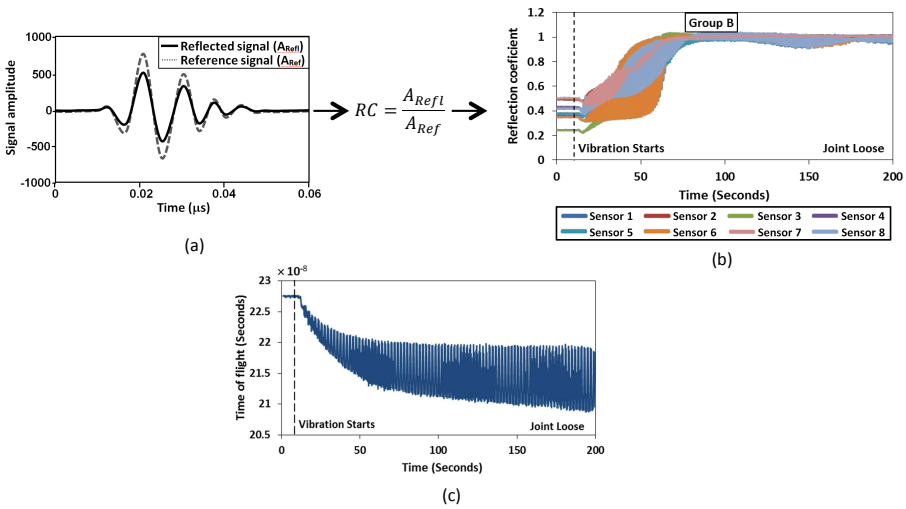

Figure 7: (a) Reflected ultrasound in time domain, (b) Dynamic reflection coefficient and (c) Dynamic time of flight measurements at 50 Nm bolt torque and frequency of 1 Hz with oscillation effect.

The figures show changes during the test, characterised by oscillation in the measurement. As observed and explained in the earlier studies of Marshall et al. [15] and shown in Figure 8, the oscillation in the measurement of the dynamic reflection coefficient is due to the relative movement between the ultrasonic sensors and the bolt head, as a result of the displacement cycles forced upon the joint. Therefore, the oscillation on data is a measurement effect that occurs at a frequency which corresponds to that of the vibration of the bolted joint. To permit meaningful analysis of the results, the data set was filtered and the centre point measurements were extracted.

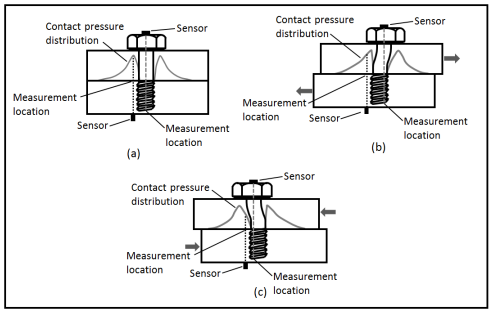

Figure 8: Relative position of the sensor and the contact pressure distribution (a) when joint components are aligned (b) when the components moved due to a tensile force of the joint (c) when the components moved due to a compressive force of the joint

Unknown
Formatted: Font:(Default) Times New Roman, 12 pt

Stephen 28/1/2016 16:14
Deleted: b

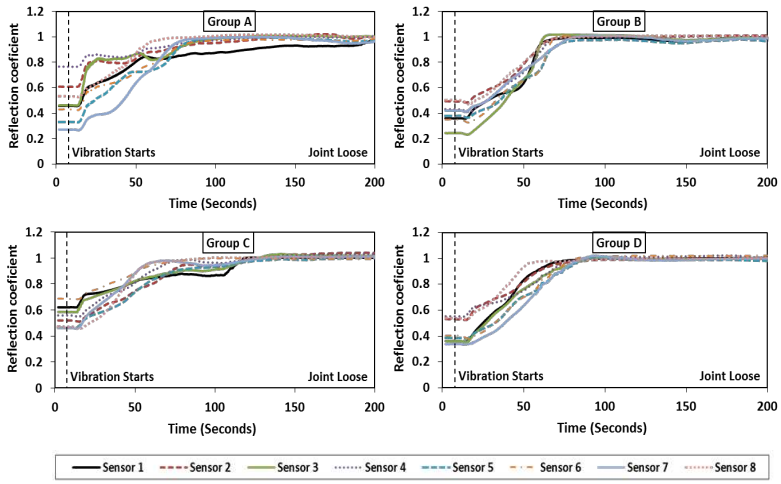

Figure 9: Dynamic reflection coefficient measurements at 50 Nm bolt torque and frequency of 1 Hz without oscillation effect

Figure 9 shows the sampled results, without the oscillation effect in the measurement, of the measured dynamic reflection coefficient at a 50 Nm bolt torque and frequency of 1 Hz for the entire 32 sensor array in four groups of eight sensors as indicated in the sensor layout in Figure 3. It should be noted that the data was not converted to contact pressure as the reflection coefficient gives a measurement of relative contact between the bolted plates and thus, a clear indication of relative loosening of the joint during the cyclic loading.

A value of dynamic reflection coefficient less than 1 indicates that the bolted plates are in contact and some portion of the ultrasonic signal is transmitted through the contact interface. As the value increases towards 1, the contact pressure at the interface of the plates decreases, which implies that the plates are separating. A value of 1 indicates that the entire ultrasonic signal has been reflected from the interface because the plates had separated and the contact pressure at the interface was zero. Also in Figure 9, it can be observed that the values of dynamic reflection coefficient of sensors with the same numerical identity in all the groups did not start at the same initial values. This can be attributed to the effect of non-uniform clamp from the bolt head as a result of the helix profile of the bolt thread and also from the plate profile irregularities of the contact surfaces, as observed in previous studies [22, 23].

Furthermore, it was observed in Figure 9 that the values of dynamic reflection coefficient cross one another as the joint loosens instead of moving parallel until their values are very close to 1. Table 2 shows that the time at which the values of dynamic reflection coefficient from consecutive sensors at the same distance from the edge of the bolt hole cross each other varies, and the variation followed the pattern of the bolt head rotation as the bolt unscrews (Figure 10). It has been observed that the pressure distribution is not symmetrically uniform around the centre hole at the interface due to non-uniform clamp from the bolt head, and the position of the peak of the contact pressure at the interface varies as the bolt head rotates during

tightening [15]. Therefore, the crossing can be attributed to movement of the peak pressure during loosening. When the bolt head rotates, the peak pressure goes around and this reduces the measured value of the dynamic reflection coefficent as it moves, leading to the observed crossing of its values.

Table 2: Time when the measured dynamic reflection coefficient cross

Sensors	Time	Sensors	Time
D5 & D1	25.3	D7 & D3	23.8
D1 & C5	44.0	D3 & C7	-
C5 & C1	48.8	C7 & C3	50.5
C1 & B5	49.0	C3 & B7	46.0
B5 & B1	50.4	B7 & B3	49.0
B1 & A5	51.0	B3 & A7	50.5
A5 & A1	56.9	A7 & A3	53.4

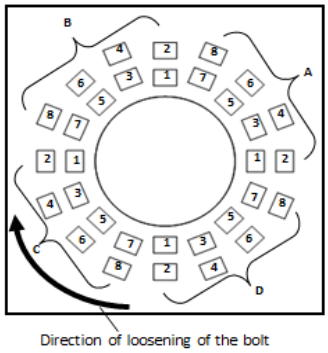

Figure 10: Direction of the bolt head rotation during loosening relative to the sensors

The average of the measured dynamic reflection coefficient of the sensors in each ring and for all the rings (i.e. from the inner ring to the outer ring) was calculated for each of the tests performed to eliminate the effects due to the thread profile and other plate irregularities. Figure 11 shows the results of the dynamic reflection coefficient (RC), dynamic reduction in time of flight (TOF) and the rotation of the bolt head during the tests. It can be seen from the figure that as the bolted joints loosen the value of the dynamic reflection coefficient increases rapidly from its initial value, followed by a gradual increase in value to approximately 1 during the vibration cycles. During this period, the values of the reduction in dynamic time of flight increases rapidly from their initial values of zero to approximately uniform values as the bolted joints loosen. Increase in the value from zero indicates a decrease in the bolt tension and loss of preload. When the dynamic time of flight attains an approximately uniform value, it implies that the joint had loosened and there was no longer any significant tension in the bolt.

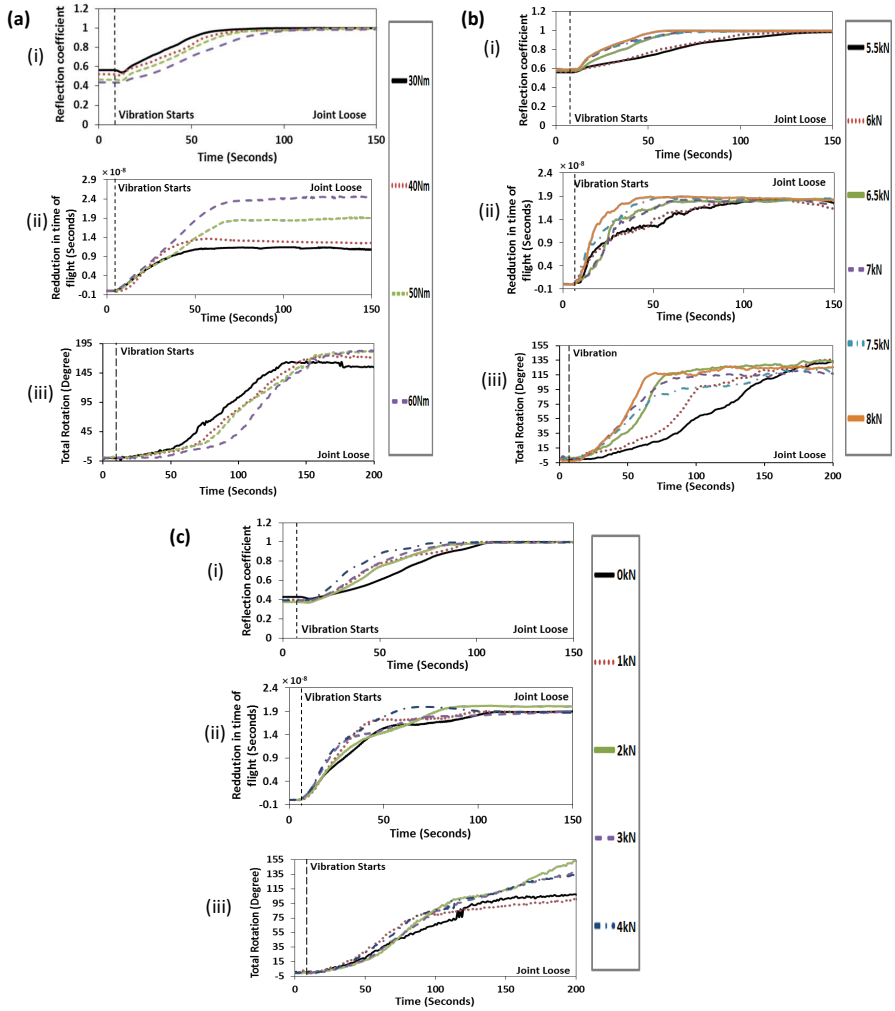

Figure 11: (i) Dynamic reflection coefficient (RC) (ii) reduction in the time of flight (TOF) and (iii) rotation of the bolt head measurements at various (a) torques, (b) cyclic shear loads and (c) transverse shear

Bolt torque and cyclic shear load

Figure 11 (a) shows that the initial value of the dynamic reflection coefficient decreases as the value of the bolt torque increases. This could be attributed to the fact that more signals are transmitted as more asperity contacts were made in the highly clamped contact zone as additional load is being applied through the tightening of the bolt [23]. Similar to observations in other studies [14, 15], the results from the monitored three areas show that the time for a complete relaxation of a given joint to occur increases as the applied bolt torque increases. In addition, the measured reduction in the dynamic time of flight shows an approximately linear relationship with bolt torque, with values of 0.10 ns, 0.12 ns, 0.16 ns and 0.21 ns measured for torques

Stephen 28/1/2016 16:11
Formatted: Font:10 pt

Stephen 28/1/2016 16:11
Formatted: Font:10 pt

Stephen 28/1/2016 16:11
Formatted: Font:10 pt

Stephen 28/1/2016 16:11
Formatted: Font:10 pt

Stephen 28/1/2016 16:11
Formatted: Font:10 pt

of 30, 40, 50 and 60 Nm respectively. As would be expected, this indicates that the bolt experienced more tension, and thus stretches more, as the bolt torque increases.

Stephen 28/1/2016 16:11
Formatted: Font:10 pt

Stephen 28/1/2016 16:11
Formatted: Font:10 pt

The results of varied cyclic shear load (Figure 11 (b)), shows that the time at which the bolted joint attained complete relaxation decreases as the applied cyclic shear load increases. The average dynamic reflection coefficient measurements attained the value of 1 at approximately 143.7 seconds, 72.1 seconds and 54.6 seconds for the cyclic shear loads of 6 kN, 7 kN and 8 kN respectively. A time value of 107.2 seconds, 65.22 seconds and 41.3 seconds was recorded for the dynamic reduction in dynamic time of flight, while a time of 170.0 seconds, 98.0 seconds and 68.0 seconds was recorded for the rotation of bolt head for the respective dynamic shear loads at the time they approximately attained uniform values. The results from each measurements show differences in relaxation time and these will be explored further during the discussion. However, the results show that the rate at which relaxation occurs increases as the applied dynamic shear load increases.

Transverse side load

In Figure 11 (c), the three measurements show that there was a steady reduction in the time of loosening as the transverse load increases. The measured dynamic reflection coefficient reaches a value of 1 at approximately 128.2 seconds, 97.7 seconds, 92.6 seconds, 88.7 seconds and 78.6 seconds. The time recorded for both the measured dynamic reduction in time of flight and rotation of the bolt head during the tests followed the same pattern as the reflection coefficient. These are indications that the rate at which loosening occurs increases as the applied transverse shear load increases.

Discussion

Results profile and phases of loosening

In the results, the value of dynamic reflection coefficient increases from a value of less than 1 when the bolted plates were in contact to a value of 1 when they were separated (Figure 12). During this period, the reduction in time of flight increases from an initial value of zero to an almost uniform value. Since both the extension in the bolt and contact pressure have a close relationships to joint load, the shapes of the two graphs in Figure 12 (a) are similar, with each showing identical phases of relaxation of the bolted joint.

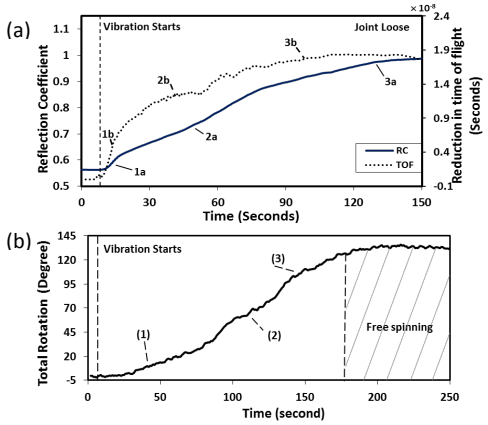

Figure 12: (a) Dynamic reflection coefficient measurements (RC) and reduction in the time of flight (TOF), and (b) Rotation of the bolt head of 5.5 kN dynamic shear loads at a frequency of 1 Hz

As shown, loosening of bolted joints exhibits phase changes that can be grouped into three stages: an initial very rapid loosening, followed by less rapid loosening and lastly, a gradual loosening. The loosening process could be compared to the illustration by Bickford [26] of the sequence by which shear joint fails in response to external loads (Figure 13(a)): the first stage involves elastic deformation of the bolted joint components, followed by the clamped components slipping relatively to one another, leading to greater interaction with the bolt after the friction at the interface has been overcome. Next additional elastic and plastic deformation occur respectively, before eventual failure. In the case of loosening due to dynamic shear load (Figure 13(b)), stage 1 involves a quick reduction of tension in the bolt and fast separation of the clamped interface, and this could be attributed to a rapid slip between the threads of the bolt and that of the mating component.

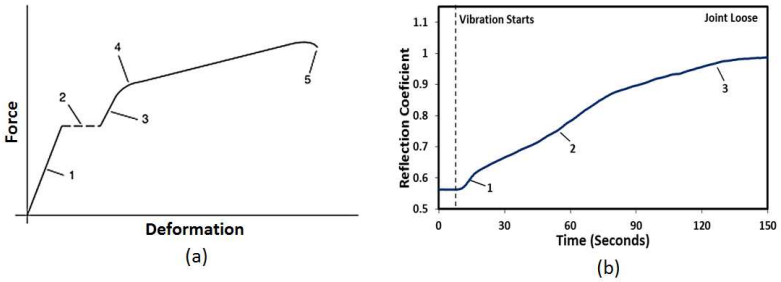

Figure 13: (a) Illustration of the sequence by which shear joint fails in response to external loads [26] and (b) Three-stage self-loosening sequence of bolted joints in the present study

The value of reflection coefficient and reduction in time of flight increases less rapidly in stage 2. The interactions between the clamped members and the bolt increased in this stage. This introduced further bending of the bolt and the gross slip at the bolt head, and the consequent rotation of the bolt head (as shown in Pai and Hess [14]). Once the friction at the interfaces have been overcome due to a substantial relaxation of the bolt tension and contact pressure at the interface, the effect of the dynamic shear force, assisted by the thread profile, is more concentrated on unscrewing the bolt in the later part of this stage. This corresponds to

stage 1 and stage 2 under the rotation of the bolted head (Figure 12(b)) where there is a gradual and later rapid increase in rotation. This stage also is the same as stages 2 and 3 under the Bickford illustration. At the end of stage 2, the results show that a high percentage of the joint preload has been lost. The last phase of the loosening process (stage 3) exhibited a gradual increase in the measured values. This phase compensates for the effect of the rundown of the bolt and alignment of the members during the tightening process of the bolted joint.

Initiation of loosening and ratcheting

Figure 14 shows the percentage change in the reflection coefficient, bolt rotation and length change for the joint over the first 30 seconds. No rotation was visible until 25 seconds when the bolt head showed a 2% change, at which the time of flight and reflection coefficient indicated a change of 50% and 20% respectively. This indicates that substantial relaxation had occurred before the observed rotation of the bolt head. It should be noted that the reflection coefficient has a non-linear inverse relationship with the contact pressure, which in turn depends on the location on the surface. Conversely, the time of flight and the rotation of bolt head are directly related to the joint load, meaning the different measurements show different percentage changes as loosening progresses. Considering these results, the decrease in bolt tension without the rotation of the bolt head implies relative movement (localized slip) occurred between the mating threads.

This result is consistent with Yanyao Jiang et al. [27], who modelled the early stage of loosening, and showed that the loss in preload is caused by localized cyclic plastic deformation (cyclic strain ratcheting) of the bolt. With regards to the observed relative lag in the time in the commencement of changes from the three monitored areas in the present study, the results show that when the bolted joint is subjected to cyclic shear loading, loosening commenced by relaxation of tension in the fastener, followed by separation of the interface of the bolted components and lastly, by the gross slip (rotation) of the bolt head. Therefore, the relaxation of the tension in the bolt at the early stage is a validation of the existence of the cyclic strain ratcheting at the mating threads of the bolt which is responsible for loss of preload and the consequent separation of clamped interface during the vibration loosening of bolted joints.

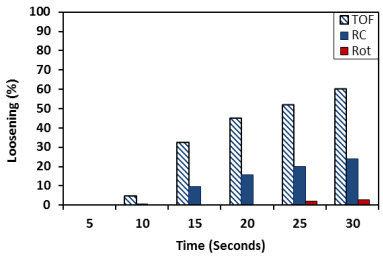

Figure 14: Dynamic RC, reduction in TOF and rotation of the bolt head measurements in the first 30 seconds of vibration test

In addition, in contrast to the classical theory that loosening starts with transverse complete slip of the bolt head surface, the observation in this study clearly shows that self-loosening occurred prior to the bolt head

Stephen 28/1/2016 15:31
Formatted: Indent: Left: 1.5 cm, Hanging: 1.5 cm, Space After: 6 pt

Stephen 28/1/2016 15:31
Formatted: Normal, Justified, Indent: Left: 0 cm, First line: 0 cm, Space After: 12 pt

Stephen 28/1/2016 15:24
Formatted: Font:(Default) +Theme Body, 10 pt

Stephen 28/1/2016 15:24
Formatted: Font:(Default) +Theme Body, 10 pt

Stephen 28/1/2016 15:24
Formatted: Font:(Default) +Theme Body, 10 pt

complete slip (rotation of bolt head). Furthermore, this is also in agreement with the studies of Pai and Hess [11, 14], Izumi et al. [28], Koch et al. [29], and Dinger and Friedrich [30] which observed that critical loosening appears prior to the bolt head slip.

Differential loosening rates across the interface

The amplitude of the contact pressure distribution at bolted interface is a function of torque while the spread is independent of the magnitude of the torque. The amplitude of the peak increases with an increase in torque (Figure 15b), but the position of the peak and the spread are driven by the effect of the stress concentration factor from the edge of bolt hole and the bolt head, and remain unchanged even as torque increases [23]. These are highlighted in the loosening data (Figure 15a), where the observed linearity in the time to reach a 50% and 90% change in the value of reflection coefficient implies that additional load is supported by the highly clamped area of the contact zone as torque increases. Whilst the relationship between reflection coefficient and contact pressure can be determined, how the change in contact pressure relates to change in total load depends on the location on the interface. Therefore, based on the shape of the distribution, the area very close to bolt hole with high contact pressure experiences lower rate of loosening, and this effect is consistent for all the joints tested.

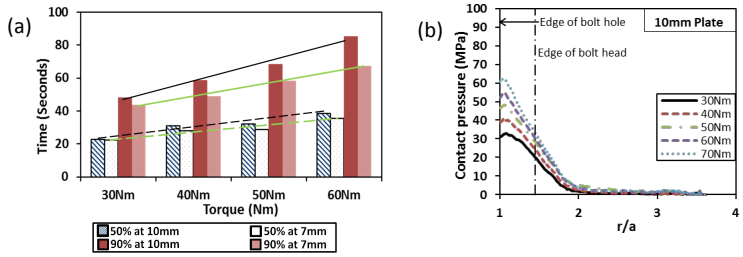

Figure 15: (a) Dynamic RC measurements at different radial distances of the bolted contact interface and (b) Normalised average contact pressure line scans [23]

Effect of cyclic shear load and transverse side load

Figure 16 shows the effect of cyclic shear and transverse loads on the loosening of bolted joints taken at 50% and 90% reduction of the changes in the measured value reflection, time of flight and rotation of the bolt head. Whilst as discussed the relationship of their measurements to total load, and therefore absolute loosening differ, they show the same overall trends. When cyclic shear load overcomes the friction at the contacts of bolted joints, then loosening will occur. Studies have shown the dependency of loosening on the amplitude of vibration of the applied load [13] [11]. Similarly, Figure 16 (a) shows that loosening depends on the magnitude of cyclic shear load. The loosening rate increases as the magnitude of the cyclic shear load increases. The measured dynamic reflection coefficient shows that at the early stage which corresponds to the non-rotational loosening, the slope of the results increases with an increase in the dynamic load. This indicates that the development of the cyclic strain ratcheting at the early stage, which lowers the resistance of bolted joints to self-loosening, depends and increases with the magnitude of the vibrating shear load.

Stephen 28/1/2016 15:24
Formatted: Font:(Default) +Theme Body, 10 pt

Stephen 28/1/2016 15:24
Formatted: Font:(Default) +Theme Body, 10 pt

Stephen 28/1/2016 15:24
Formatted: Font:(Default) +Theme Body, 10 pt

Stephen 28/1/2016 15:24
Formatted: Font:(Default) +Theme Body, 10 pt

Stephen 28/1/2016 15:32
Formatted: Space After: 6 pt

Stephen 28/1/2016 15:32
Formatted: Space After: 6 pt

Stephen 28/1/2016 15:32
Formatted: Space Before: 6 pt

Stephen 28/1/2016 15:31
Formatted: Space After: 0 pt

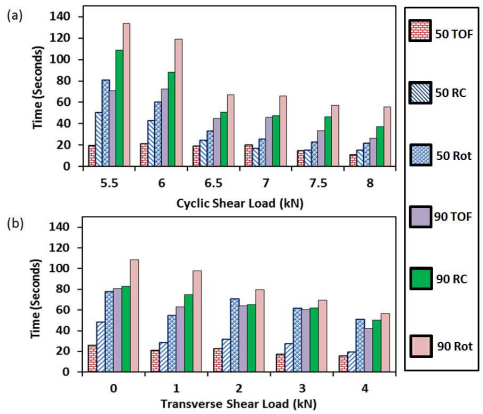

Figure 16: Dynamic RC, reduction in TOF and rotation of the bolt head measurements at 50% and 90% of loosening life for the various (a) cyclic shear loads and (b) transverse shear loads

Furthermore, the most apparent cause of loosening of bolted joints is the dynamic shear load. But when an additional shear load is constantly applied to the joint in another direction to the dynamic shear load, the results (Figure 16 (b)) show that as the magnitude of the constant shear load increases, the rate of loosening also increases even when the magnitude of applied cyclic shear load is constant. In addition, Figure 10 (b) shows that introducing and increasing the transverse shear load has a more pronounced effect on the early part of the stage 2 than any other stages of dynamic reflection coefficient and change in time of flight profiles. Once the stage 1 is accomplished the side load helps to free the clamped components of frictional force at the interfaces quickly, and subsequently, the bearing of the clamped component on the fastener introduced bending [11] and this assisted in initiating rotation of the bolt head rapidly. With the increase in the shear load, there is almost absence of the early part of the stage 2, as the stage is accomplished within a very short duration. Essentially, this result shows that additional shear load on bolted joints (for example, shear load on the rail joints and bridges due to effect of thermal stress) subjected to cyclic loading should not be ignored at the design stage, as this may introduce large errors which will affect the joint stiffness and integrity in service. It is also important to incorporate this in the design of the maintenance regime for such joints, especially if the value of the additional load periodically varies.

Conclusions

Non-intrusive methods have been used to measure the loosening of bolted joints subjected to cyclic shear loading. The following are the findings and the effects of these studied variables on the loosening of bolted joints:

- The effect of non-uniform clamping from the bolt head as a result of the helix profile of the bolt thread was observed to produce localised peak contact pressures at the bolted interface, and this localised peak contact pressure moves in the direction of the bolt head rotation when the bolt unscrews during loosening.

Stephen 28/1/2016 15:32
Formatted: Space After: 6 pt

- The measured reflected ultrasonic signals shows that the loosening of bolted joints can be grouped into three stages. The joints were observed to undergo a rapid relaxation in the first stage, followed by a period of less rapid loosening in the second stage. The first two stages accounted for a high percentage of the loss in the joint preload, while the remaining preload was lost in last stage which involves a gradual loosening of the joints. Furthermore, the higher the rate of relaxation at the early stage of loosening, the lower is the resistance of the bolted joints to vibrating induced loosening. While all the studied variables affect the early stage of loosening, the transverse shear load has pronounced effect on the early part of the stage 2 of the loosening process.
- The results show that, when a bolted joint is subjected to cyclic shear loading, the early stage of the loosening of bolted joints is characterised by cyclic strain ratcheting - loosening of the bolted joint during vibration without rotation of the bolt head. It was also observed that the rate of loosening at the bolted joint interface are not the same, but increases away from the bolt hole.
- Increasing the bolt torque reduces the loosening time, and thus increases the loosening resistance of the bolted joint. Furthermore, the rate of loosening of bolted joints depends on the magnitude of the dynamic shear load.
- When joints are subjected to constant shear load in addition to the dynamic shear load, the loosening rate increases. As the magnitude of the constant shear load increases, the rate of loosening also increases even when the amplitude of applied cyclic shear load is constant.

References

1. Khraisat, A., A. Hashimoto, S. Nomura, and O. Miyakawa, *Effect of lateral cyclic loading on abutment screw loosening of an external hexagon implant system*. The Journal of prosthetic dentistry, 2004. **91**(4): p. 326-334.
2. Kaminskaya, V. and A. Lipov, *Self Loosening of Bolted Joints in Machine Tools During Service.* Metal Cut. Mach. Tools, 1990. **12**: p. 81-85.
3. *Health and Safety Investigation Board Report-Train Derailment at Potters Bar, UK, 10 May 2002, SMIS Ref. No.: QNE/2002/02/71643, No. 04655675,2003.* p. 1-24.
4. *"Tragedia sui binari" (in Italian). Il Sole 24 Ore. January 7, 2004. Retrieved July 1, 2009.*
5. *AAIB, Air Accident Investigation Branch Report into the Crash of a Light Aircraft due to the Loss of a Stiffnut, AAIB Bulletin No: 6/2003, Ref: EW/C2002/05/03, 2006.*
6. Sase, N., K. Nishioka, S. Koga, and H. Fujii, *An anti-loosening screw-fastener innovation and its evaluation.* Journal of Materials Processing Technology, 1998. **77**(1–3): p. 209-215.
7. Cheatham, C.A., C.F. Acosta, and D.P. Hess, *Tests and analysis of secondary locking features in threaded inserts.* Engineering Failure Analysis, 2009. **16**(1): p. 39-57.
8. Goodier, J.N. and R.J. Sweeney, *Loosening by vibration of threaded fastenings.* Mechanical Engineering. 1945. 67: 798-802.
9. Sauer, J.A., D.C. Lemmon, and E.K. Lynn, *How to prevent their loosening.* Machine Design, 1950. **22**: p. 133-139.
10. Hemmye, J. *Partial slip damping in high strength friction grip bolted joints, Proceedings of the Fourth International Conference of Mathematical Modeling, Pergamon Press, New York*. 1983.
11. Pai, N.G. and D.P. Hess, *Three-dimensional finite element analysis of threaded fastener loosening due to dynamic shear load.* Engineering Failure Analysis, 2002. **9**(4): p. 383-402.

12. Jiang, Y., M. Zhang, and C.-H. Lee, *A Study of Early Stage Self-Loosening of Bolted Joints.* Journal of Mechanical Design, 2003. **125**(3): p. 518.
13. Junker, G., *New criteria for self-loosening of fasteners under vibration.* SAE Paper 690055, 1969.
14. Pai, N.G. and D.P. Hess, *Experimental study of loosening of threaded fasteners due to shear loads.* Journal of Sound and Vibration, 2002. **253**(3): p. 585-602.
15. Marshall, M.B., R. Lewis, T. Howard, and H. Brunskill, *Ultrasonic measurement of self-loosening in bolted joints.* Proceedings of the Institution of Mechanical Engineers, Part C: Journal of Mechanical Engineering Science, 2011.
16. Finkelston, R.J., *How much shake can bolted joints take.* Machine Design, 1972(44): p. 122-125.
17. Mascarenas, D.L., K.M. Farinholt, M.D. Todd, and C.R. Farrar, *A low-power wireless sensing device for remote inspection of bolted joints.* Proceedings of The Institution of Mechanical Engineers Part G-journal of Aerospace Engineering, 2009. **223**(5): p. 565-575.
18. Bhalla, S., P.A. Vittal, and M. Veljkovic, *Piezo-impedance transducers for residual fatigue life assessment of bolted steel joints.* Structural Health Monitoring, 2012. **11**(6): p. 733-750.
19. Thrassos Panidis, P., I. Pavelko, V. Pavelko, S. Kuznetsov, and I. Ozolinsh, *Bolt-joint structural health monitoring by the method of electromechanical impedance.* Aircraft Engineering and Aerospace Technology, 2014. **86**(3): p. 207-214.
20. Chesson Jr, E. and W.H. Munse, *Studies of the behavior of high-strength bolts and bolted joints, Bulletin 469,University of Illinois, Experimental Station.* 1964.
21. Sakai, T., *The friction coefficient of fasteners.* Bulletin of the JSME, 1978. **21**: p. 333-340.
22. Marshall, M.B., R. Lewis, and R.S. Dwyer-Joyce, *Characterisation of contact pressure distribution in bolted joints.* Strain, 2006. **42**(1): p. 31-43.
23. Stephen, J., M. Marshall, and R. Lewis, *An investigation into contact pressure distribution in bolted joints.* Proceedings of the Institution of Mechanical Engineers, Part C: Journal of Mechanical Engineering Science, 2014. **228**(18): p. 3405-3418.
24. Gonzalez, R.C., R.E. Woods, and S.L. Eddins, *Digital Image Processing Using Matlab*. 1st ed. 2006, India: Dorling Kindersley Pvt Ltd.
25. Shigley, J.E. and C.R. Mischke, *Mechanical Engineering Design*. 6th ed. 2001: McGraw-Hill, Singapore.
26. Bickford, J.H., *An introduction to the design and behaviour of bolted joints*. 1990, New York: Marcel Dekker Inc.
27. Jiang, Y., M. Zhang, T.-W. Park, and C.-H. Lee, *An Experimental Study of Self-Loosening of Bolted Joints.* Journal of Mechanical Design, 2004. **126**(5): p. 925-931.
28. Izumi, S., T. Yokoyama, A. Iwasaki, and S. Sakai, *Three-dimensional finite element analysis of tightening and loosening mechanism of threaded fastener.* Engineering Failure Analysis, 2005. **12**(4): p. 604-615.
29. Koch, D., C. Friedrich, and G. Dinger. *Simulation of rotational self-loosening of bolted joints*. in *NAFEMS Seminar-FEM Idealisation of Joints*. 2010.
30. Dinger, G. and C. Friedrich, *Avoiding self-loosening failure of bolted joints with numerical assessment of local contact state.* Engineering Failure Analysis, 2011. **18**(8): p. 2188-2200.